nature chemistry

SUPPLEMENTARY INFORMATION

DOI: 10.1038/NCHEM.2449

Microscopic origin of chiral shape induction in achiral crystals

Wende Xiao[1,2], Karl-Heinz Ernst[1,3], Krisztian Palotas[4], Yuyang Zhang[2], Emilie Bruyer[5], Lingqing Peng[6], Thomas Greber[7], Werner A. Hofer[8], Lawrence T. Scott[6], & Roman Fasel[1,9*]

[1] Empa, Swiss Federal Laboratories for Materials Science and Technology, Überlandstrasse 129, 8600 Dübendorf, Switzerland.

[2] Institute of Physics, Chinese Academy of Sciences, 100190 Beijing, China

[3] Department of Chemistry, University Zürich, Zürich, Switzerland

[4] Department of Theoretical Physics, Budapest University of Technology and Economics, Hungary

[5] CNR-SPIN, I-67010, L'Aquila, Italy

[6] Department of Chemistry, Merkert Chemistry Center, Boston College, Chestnut Hill, MA 02467-3860, USA

[7] Department of Physics, University Zürich, Zürich, Switzerland

[8] School of Chemistry, Newcastle University, Newcastle, UK

[9] Department of Chemistry and Biochemistry, Universität Bern, Bern, Switzerland

[*] email: roman.fasel@empa.ch

Contents

1) Additional analysis

a) Analysis of hemifullerene C 1*s* X-ray Photoelectron Diffraction (XPD) data

Supplementary Figure 1a shows the C 1*s* XPD data acquired from hemifullerene adsorbed on Cu(110). C 1*s* XPD patterns were measured in forward scattering condition (E_{kin}=626 eV) and are represented as stereographic projections in grey scale (white: maximum intensity). The centre corresponds to normal emission and the border to the maximum grazing angle measured (88°). The orientation of the substrate, as determined by an XPD pattern of the Cu 3*p* core level, is also indicated. In order to enhance the statistical accuracy, the experimental patterns have been azimuthally averaged, exploiting the twofold symmetry of the substrate. This procedure did not produce any extra features with respect to the raw data.

Photoelectron diffraction patterns $I(\vartheta,\varphi)$ from the adsorbed hemifullerene C 1*s* level were acquired at room temperature for extensive sets of emission angles (ϑ,φ), with $0\leq\vartheta\leq88°$ and $0\leq\varphi\leq360°$. Data sets from four different sample preparations were analysed, determined to be equivalent and thus merged into the averaged data set $I^{EXP}(\vartheta,\varphi)$ shown in Supplementary Figure 1a.

For further analysis and comparison with simulations, this pattern was expanded in terms of spherical harmonics, resulting in the experimental set of multipole coefficients a_{lm}^{EXP}, with l=0,1,...,60 and m=-l,..,+l:

$$I^{EXP}(\vartheta,\varphi)=\sum_{l,m}a_{lm}^{EXP}\cdot Y_{lm}(\vartheta,\varphi) \quad (1)$$

where the multipole coefficients a_{lm} are obtained from

$$a_{lm}^{EXP}=\frac{1}{4\pi}\int\chi^{EXP}(\vartheta,\varphi)\cdot Y_{lm}^{*}(\vartheta,\varphi)\,d\Omega \quad (2)$$

Here, the $Y_{lm}^{*}(\vartheta,\varphi)$ are the complex conjugates of the spherical harmonics, and $\chi^{EXP}(\vartheta,\varphi)$ is the oscillatory part of the diffraction pattern obtained by normalization with respect to the average intensity $\langle I(\vartheta)\rangle_{\varphi}$ for each polar angle theta:

$$\chi(\vartheta,\varphi)=\frac{I(\vartheta,\varphi)-\langle I(\vartheta)\rangle_{\varphi}}{\langle I(\vartheta)\rangle_{\varphi}} \quad (3)$$

In order to determine the molecular orientation(s) of the hemifullerene on Cu(110) giving rise to the experimentally obtained XPD pattern $I^{EXP}(\vartheta,\varphi)$, a simulated diffraction pattern $I^{SSC}(\vartheta,\varphi)$ for the *M*-enantiomer of hemifullerene adsorbed with its C_3 symmetry axis perpendicular to the surface was computed by means of single-scattering cluster (SSC) theory[1] (Supplementary Figure 2). Again, the pattern was expanded in terms of spherical harmonics, resulting in the calculated set of multipole coefficients a_{lm}^{SSC}, with l=0,1,...,60 and m=-l,..,+l:

$$I^{SSC}(\vartheta,\varphi)=\sum_{l,m}a_{lm}^{SSC}\cdot Y_{lm}(\vartheta,\varphi) \quad (4)$$

where the multipole coefficients a_{lm} are obtained from

$$a_{lm}^{SSC}=\frac{1}{4\pi}\int\chi^{SSC}(\vartheta,\varphi)\cdot Y_{lm}^{*}(\vartheta,\varphi)\,d\Omega \quad (5)$$

$\chi^{SSC}(\vartheta,\varphi)$ is the oscillatory part of the calculated diffraction pattern obtained by normalization with respect to the average intensity $\langle I(\vartheta)\rangle_{\varphi}$ for each polar angle ϑ (eq. 3).

The agreement between experiment $I^{EXP}(\vartheta,\varphi)$ and calculation $I^{SSC}(\vartheta,\varphi)$ was quantified by means of a reliability factor (*R* factor) R_{MP} based on the space of multipole expansion coefficients[2]:

$$R_{MP} = \sum_{l=0}^{l_{max}} \sum_{m=-l}^{l} \left| a_{lm}^{SSC} - a_{lm}^{EXP} \right| / \left| a_{lm}^{SSC} + a_{lm}^{EXP} \right| \quad (6)$$

Setting l_{max} to 60 was sufficient to reproduce all fine structure present in the data.

In the standard approach to XPD-SSC analysis, calculations for a wide range of molecular orientations are performed and compared to experiment, until best agreement is found. In the present case of two coexisting molecular orientations, this is computationally not feasible, and we thus developed an alternative approach based on rotations in the space of multipole expansion coefficients, as outlined below.

We start by considering the general situation where more than one (inequivalent) molecular orientation must be considered, i.e. coexisting molecular orientations must be included in the analysis. We consider a case with $nOrient$ coexisting molecular orientations. Each orientation contributes with a weight w_i to the total pattern, thus the pattern from all coexisting orientations is obtained by incoherent summation:

$$I^{SSC}(\vartheta,\varphi) = \sum_{i=1}^{nOrient} w_i \cdot I_i^{SSC}(\vartheta,\varphi) \quad (7)$$

with

$$w_1 + w_2 + \ldots + w_{nOrient} = 1 \quad (8)$$

Instead of doing full-featured SSC calculations for all molecular orientations, only a single SSC calculation I^{4piSSC} is performed for an isolated, single molecule in a particular "standard" molecular orientation, but over the full 4π hemisphere of emission angles. Simulated diffraction patterns for arbitrarily oriented molecules can now be obtained from this "standard" full 4π SSC calculation by simply rotating I^{4piSSC} by the appropriate Euler angles $\alpha\beta\gamma$. The assumption here is that the molecular conformation is determined by intramolecular interactions and not by molecule-substrate interactions, i.e. that the molecular skeleton does not significantly relax when it is facing the substrate under slightly different orientations. This (implicit) assumption has previously been used successfully for the related cases of C_{60}[3] and corannulene[4] adsorbed on the same Cu(110) substrate, and is expected to be valid for hemifullerene as well.

To further save computation time, the rotation of the computed full 4π SSC pattern can also be done entirely in the space of multipole coefficients a_{lm}^{4piSSC} obtained from the multipole expansion of I^{4piSSC}:

$$I^{4piSSC}(\vartheta,\varphi) = \sum_{l,m} a_{lm}^{4piSSC} \cdot Y_{lm}(\vartheta,\varphi) \quad (9)$$

Rotation of I^{4piSSC} by the Euler angles $\alpha\beta\gamma$ (rotation operation $R^{\alpha\beta\gamma}$) gives the rotated diffraction pattern I^{rotSSC}:

$$I^{4piSSC}(\vartheta,\varphi) = \sum_{l,m} a_{lm}^{4piSSC} \cdot Y_{lm}(\vartheta,\varphi) \xrightarrow{R^{\alpha\beta\gamma}} I^{rotSSC}(\vartheta,\varphi) = \sum_{l,m} a_{lm}^{rotSSC} \cdot Y_{lm}(\vartheta,\varphi) \quad (10)$$

with new multipole coefficients a_{lm}^{rotSSC} that are obtained from the original coefficients a_{lm}^{4piSSC} via spherical harmonics rotation[5]:

$$a_{lm}^{rotSSC} = Z_\gamma Y_\beta Z_\alpha a_{lm}^{4piSSC} \quad (11)$$

where Z_α is a rotation about the z-axis, Y_β a rotation about the y-axis, and Z_γ a rotation about z again.

To further simplify calculation of the rotated multipole coefficients, the rotation by the Euler angles $\alpha\beta\gamma$ can also be expressed by a combination of rotations around the z-axis and ±90° rotations around the x-axis, which is computationally very efficient:

$$a_{lm}^{rotSSC} = Z_\gamma X_{-90°} Z_\beta X_{90°} Z_\alpha a_{lm}^{4piSSC} \quad (12)$$

In the present case of two coexisting molecular orientations $\alpha_1\beta_1\gamma_1$ and $\alpha_2\beta_2\gamma_2$ of hemifullerene on Cu(110), with relative weights of w_1 and w_2, we can thus easily obtain the multipole coefficients a_{lm}^{SSC} of the corresponding diffraction pattern from the ones of the hemifullerene in standard orientation (3-fold rotational axis perpendicular to the surface, bowl-opening facing away from the substrate, see Supplementary Figure 2) a_{lm}^{4piSSC}:

$$a_{lm}^{SSC}(w_1,\alpha_1,\beta_1,\gamma_1,w_2,\alpha_2,\beta_2,\gamma_2) = \\ w_1 \cdot Z_{\gamma_1} X_{-90°} Z_{\beta_1} X_{90°} Z_{\alpha_1} a_{lm}^{4piSSC} + w_2 \cdot Z_{\gamma_2} X_{-90°} Z_{\beta_2} X_{90°} Z_{\alpha_2} a_{lm}^{4piSSC} \quad (13)$$

For comparison to experiment, the presence of equal amounts of *M*- and *P*-hemifullerene enantiomers as well as the 2-fold rotational symmetry of the substrate surface are taken into account by applying mirror symmetry and 2-fold rotational symmetry to the diffraction pattern (see Supplementary Figures 2 and 3), which can again be done directly on the multipole coefficients.

To avoid being trapped in local minima, minimization of the *R* factor (eq. 6) was performed with a differential evolution algorithm[6] as implemented in the Genetic Curvefitting extension "GenCurveFit XOP" [7] to the IGOR Pro software[8]. Multiple starting guesses were used to ensure identification of the global best fit.

The resulting best-fit SSC calculation is shown in Supplementary Figure 1b. There is excellent agreement with the experimental data (Supplementary Figures 1a, 3d,e), as also confirmed by the significantly improved *R* factor of 0.22 compared to values between 0.25 and 0.37 for the cases where only a single orientation is taken into account (Supplementary Figure 3). The two best-fit orientations are sketched in Supplementary Figure 1c-f. One third of the hemifullerene molecules take an orientation with their 3-fold symmetry axis tilted by 10° away from the surface normal along the $[1\bar{1}2]$ direction

(indicated by dashed black arrow in 1c). This tilt brings the 6-6 bond between the central C6 ring and an adjoining C6 ring closest to the substrate surface (highlighted in red in 1c), and results in different heights above the surface for the three outermost C6 rings. This height difference amounts to 1.1 Å, and for the *M*-enantiomer of hemifullerene defines a *clockwise* sequence from highest (1) to middle (2) to lowest (2) C6 rings in a top view such as the one given in Supplementaryl Figure 1c (anti-clockwise for the *P*-enantiomer). From comparison of this configuration and its minority appearance (~$^1/_3$) with the STM results, we attribute it to the hemifullerene adsorbed on Cu(110) terraces. The majority species (~$^2/_3$) exhibits a significantly larger tilt of 18° away from the high-symmetry configuration, as illustrated in Supplementary Figure 1e,f. Its 3-fold symmetry axis is inclined by 18° along the $[1\bar{1}0]$ direction (indicated by dashed black arrow in 1e), which brings the 5-6 bond between the central C6 ring and the adjoining C5 ring closest to the surface (highlighted in red in 1e). For this majority configuration, the sequence of highest (1) to middle (2) to lowest (2) C6 ring is *anti-clockwise* for *M*-hemifullerene, and with a significantly larger height difference of 1.9 Å. It clearly corresponds to the hemifullerenes observed to decorate step edges in STM images.

A comparison between the best-fit molecular orientations of *M*-hemifullerene at the step edge as determined from the XPD-SSC analysis and the minimum energy configuration from the extensive simulated annealing molecular dynamics DFT calculations is shown in Supplementary Figure 6. Despite the complexity of the system under investigation, with many degrees of freedom, the agreement between the two results is excellent. From both approaches, we find that the *M*-hemifullerene faces the Cu substrate with a 5-6 bond, with almost identical values for the tilt angle of its 3-fold symmetry axis (experiment: 18°; calculation: 20°), identical tilt directions (tilting around the 5-6 bond) and azimuthal orientations (3.5° difference between experiment and calculation).

We note that the XPD measurements were performed at room temperature where the molecules on terraces were too mobile to be imaged by STM. The difference in temperature between XPD and STM experiments should, however, have no influence on the validity of the method. According to the transition state theory of diffusion, molecular diffusion on a solid substrate proceeds with the molecules going over a barrier between two identical, energetically most favourable binding configurations. The residence time in the transition state - and only there a different configuration than the one determined by XPD can be expected - will be negligible compared to the residence time in the stable binding sites. Therefore, XPD collects photoelectrons essentially only from molecules residing in the stable adsorption sites, with the corresponding results thus being equally valid for the low temperature situation where diffusion is inhibited.

2) Additional data

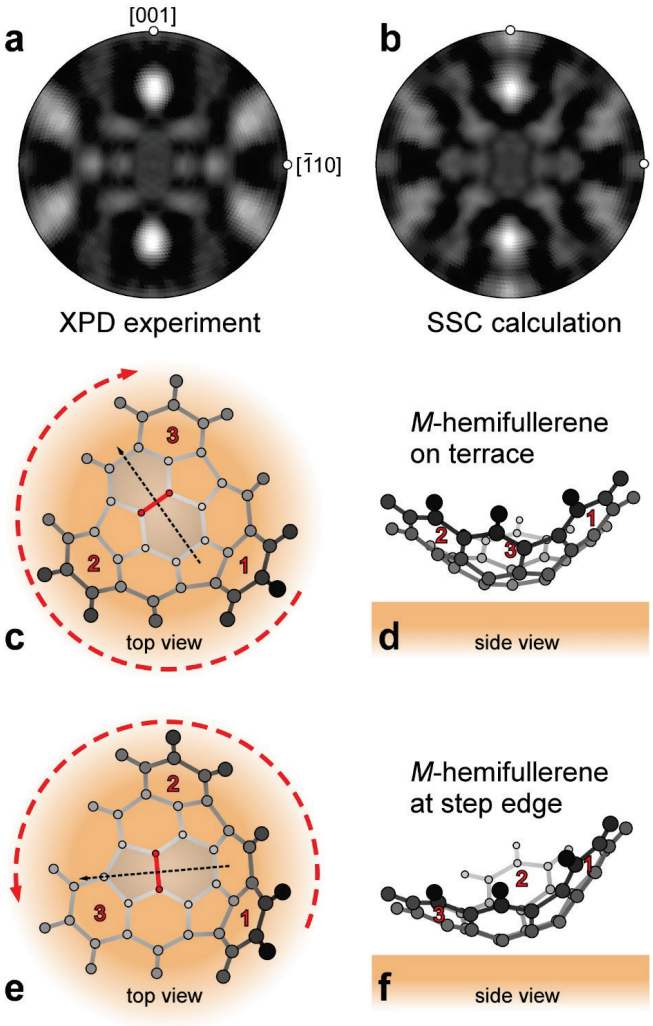

Supplementary Figure 1 | XPD analysis of molecular orientations. (**a**) C1*s* XPD pattern acquired with the sample held at room temperature. (**b**) Simulated XPD pattern from single-scattering cluster (SSC) calculations accurately reproducing the experimental pattern. *R* factor analysis discloses two different adsorption configurations ("on-terrace" and "at-step-edge"), both demonstrating that the molecular C_3 axis is significantly inclined away from the surface normal. The best-fit molecular ratio of hemifullerene adopting the on-terrace and at-step-edge configurations is about 1:2, in good agreement with STM observations. (**c**,**d**) On-terrace adsorption configuration of *M*-hemifullerene on Cu(110) according to the SSC calculations. The tilt of the *M*-enantiomer by 10° along the [1 $\bar{1}$ 2] direction (dashed black arrow) brings the 6-6 bond highlighted in red closest to the surface, and results in a clockwise sequence from highest (1) to middle (2) to lowest (3) C6 rings in a top view, as indicated by the red dashed arrow. (**e**,**f**) At-step-edge adsorption configuration of *M*-hemifullerene on Cu(110). The tilt of the *M*-enantiomer by 18° along the [1 $\bar{1}$ 0] direction (dashed black arrow) brings the 5-6 bond highlighted in red closest to the surface, and results in a counterclockwise intensity decrease sequence of the three outmost C6 rings.

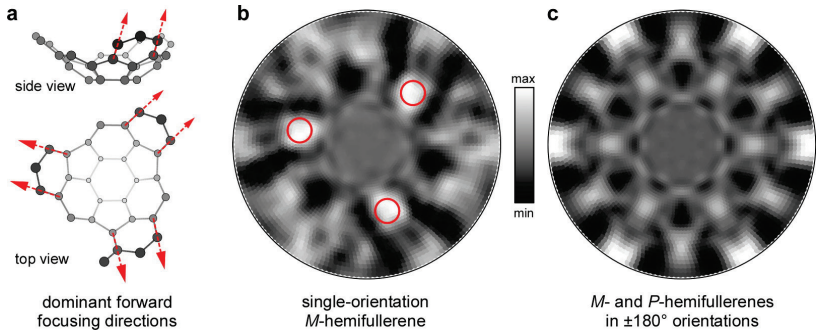

Supplementary Figure 2 | Photoelectron diffraction from surface-adsorbed hemifullerene. (**a**) Illustration of the carbon skeleton of a *M*-hemifullerene molecule with its 3-fold symmetry axis perpendicular to the substrate surface, with red arrows highlighting the C-C bond directions producing the dominant forward focusing maxima in the C 1*s* photoelectron diffraction pattern. The carbon atoms are color coded according to their distance from the viewer, with darker grey tones corresponding to closer distances. (**b**) Simulated XPD pattern (SSC calculation) for a single *M*-hemifullerene oriented as shown in (**a**). Red circles highlight the three prominent intensity maxima due to forward scattering along the directions indicated by red arrows in (**a**). (**c**) SSC calculation taking into account both *M*- and *P*-hemifullerene enantiomers as well as the 2-fold rotational symmetry of the substrate surface.

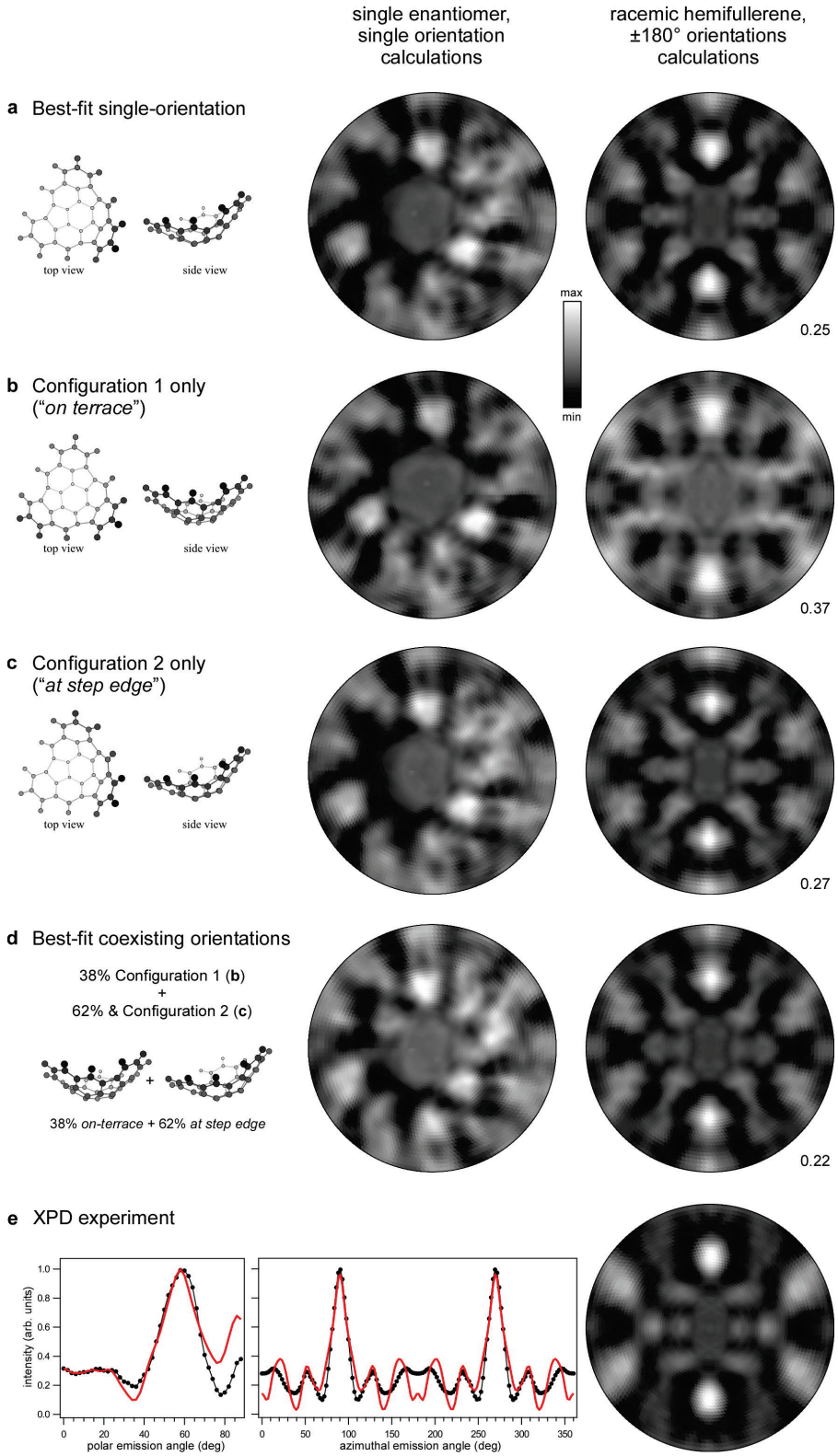

Supplementary Figure 3 | SSC calculations for various hemifullerene orientations. (a-d) SSC calculations for different configurations. The left column gives a sketch of the corresponding molecular orientation(s). The middle and right columns show the resulting SSC calculations for the (artificial) case of enantiopure *M*-hemifullerene with a single azimuthal orientation (middle) and for the realistic

case with both *M*- and *P*-enantiomers (mirror symmetry) as well as 2-fold rotational symmetry due to the Cu(110) substrate (right). The numbers at the bottom right of the SSC patterns give the *R* factor R_{MP} (equation 6) quantifying the agreement between the SSC calculation and the experimental XPD pattern. (**e**) Experimental C 1*s* XPD pattern (right), and comparison of polar cuts (left) and azimuthal cuts (middle) through its most prominent maxima with the corresponding cuts from the best-fit SSC calculation shown in (**d**). Black dots: experimental data; red line: SSC calculation.

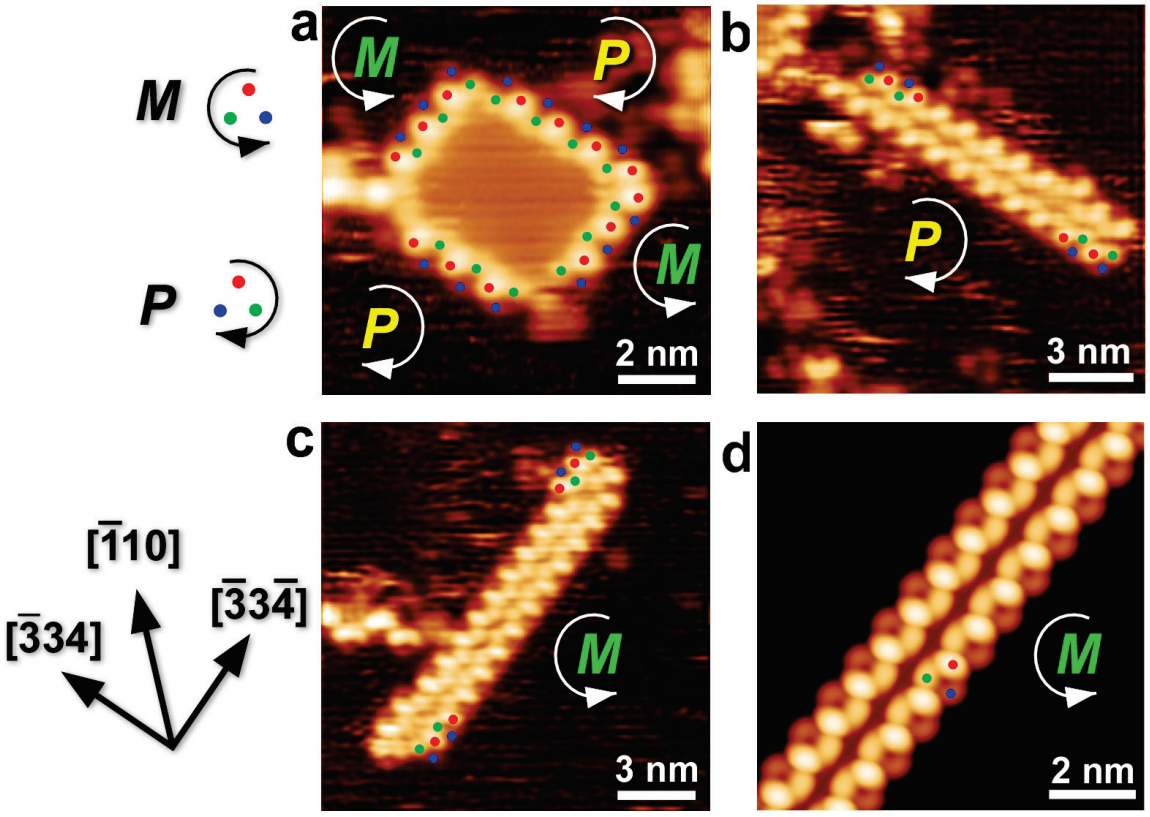

Supplementary Figure 4 | Enantioselective step decoration of 2D Cu islands and Cu adatom nanowires. Red, green and blue dots indicate the hemifullerene's outer C6 rings with highest, middle and lowest apparent heights, respectively. A counter-clockwise height decrease of the three C6 rings identifies an *M*-enantiomer, whereas a clockwise height decrease is assigned to the *P*-enantiomer. (**a**)-(**c**) Steps and wires running parallel to the [$\bar{3}3\bar{4}$] direction are decorated with *M*-enantiomers, those running parallel to the [$\bar{3}34$] direction are decorated with *P*-enantiomers (T = 300 K, U = –2.0 V; I = 23 pA for image a, U = –2.4 V; I = 35 pA for images **b**,**c**). (**d**) DFT-based STM simulation of a *M*-hemifullerene stabilized Cu adatom nanowire running along [$\bar{3}3\bar{4}$]. The sequence of highest, to middle, to lowest protrusion in STM appearance of a *M*-hemifullerene is indicated by the coloured dots, and is in excellent agreement with experimental observations.

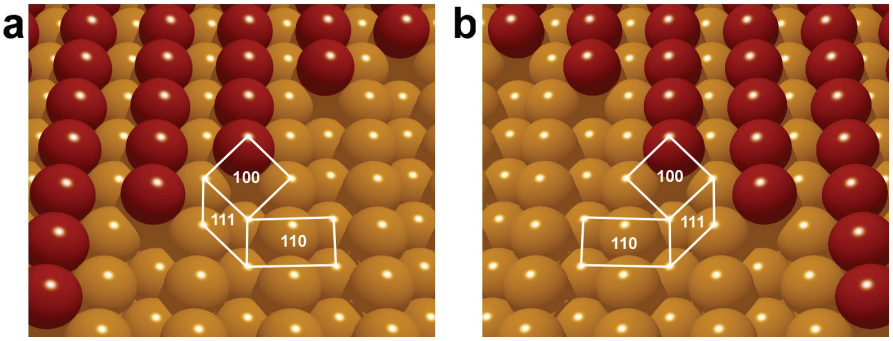

Supplementary Figure 5 | Definition of *R*- and *S*-kinks. The sequence of facets from (100) via (110) to (111) at the kink is either clockwise (*R*-kink, **a**) or counter clockwise (*S*-kink, **b**).

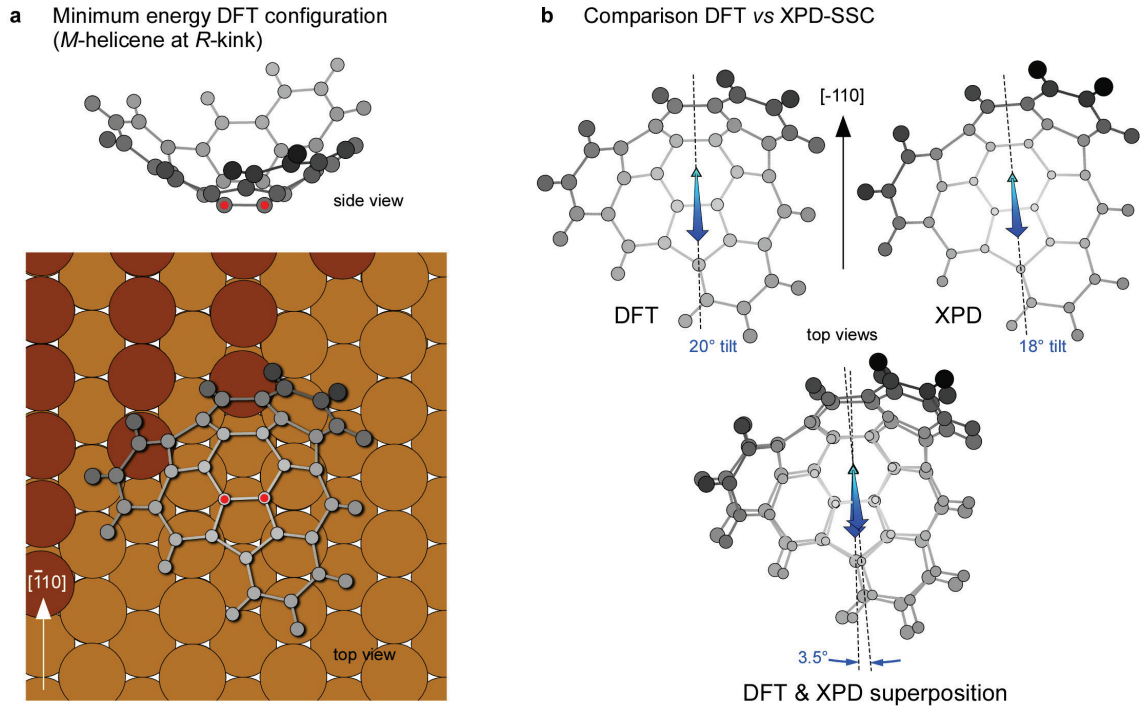

Supplementary Figure 6 | Comparison of molecular orientation at the kinked step edge as obtained from DFT and XPD. (**a**) Illustration of the minimum energy adsorption configuration of *M*-hemifullerene on Cu(110) as obtained from the DFT calculations. The 3-fold axis of the molecule is tilted by 20° along the [1 $\bar{1}$ 0] direction which brings the 5-6 bond highlighted in red closest to the surface. The carbon atoms are color coded according to their distance from the viewer, with darker grey tones corresponding to closer distances. (**b**) Comparison of the molecular orientation of *M*-hemifullerene in the minimum energy DFT configuration (left) with the one of the majority species obtained from the XPD-SSC analysis (right). A direct superposition of the two is shown at the bottom.

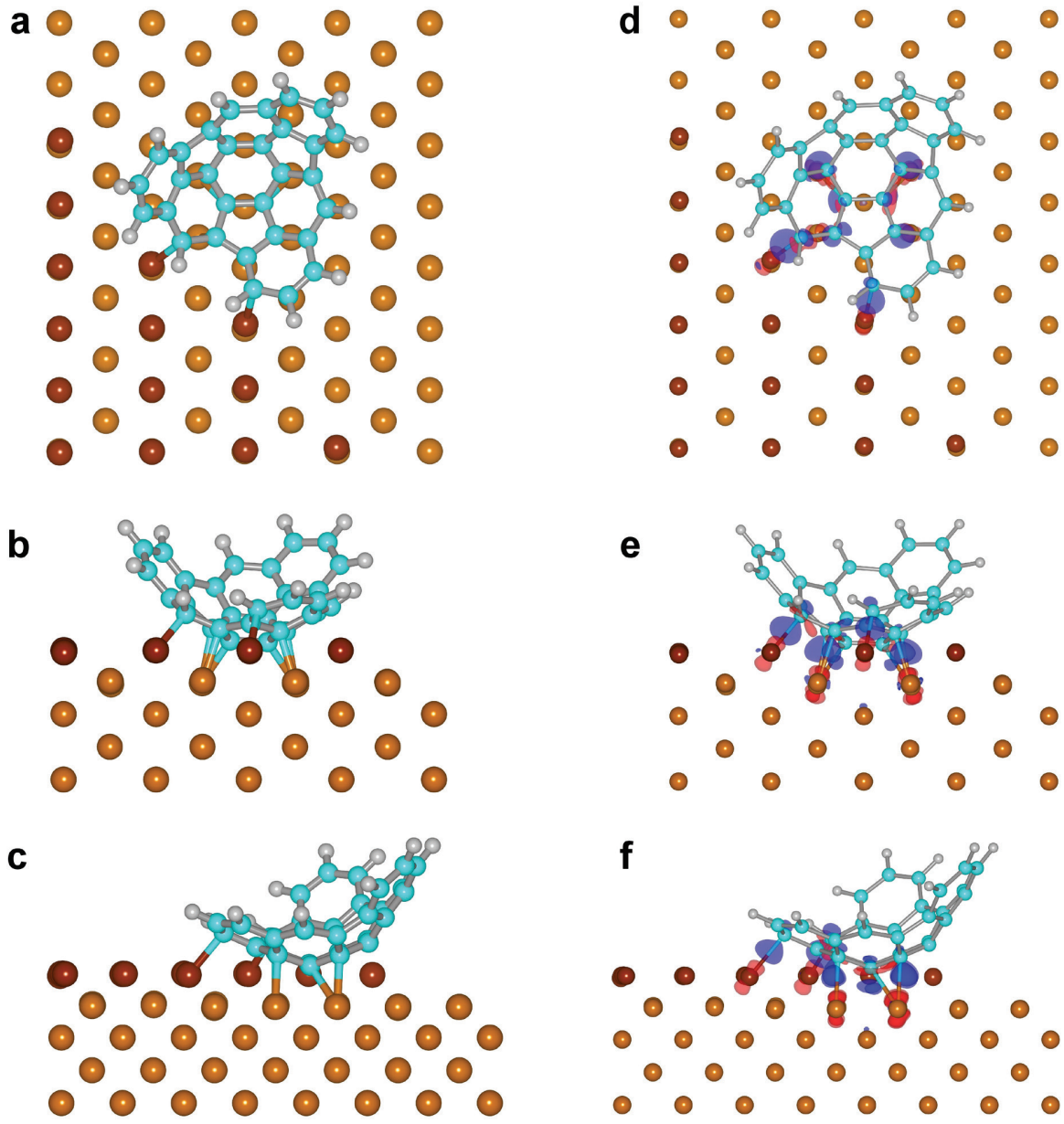

Supplementary Figure 7 | Optimized configuration of *M*-hemifullerene at the *S*-kink. Top (**a**), front (**b**) and side (**c**) views of *M*-hemifullerene bound to an *S*-kink as obtained by DFT calculations. The bonds are identified via charge density distribution calculations (**d**-**f**). Charge depletion is marked in red, charge accumulation in blue with a contour value of 0.06 e/Å^3.

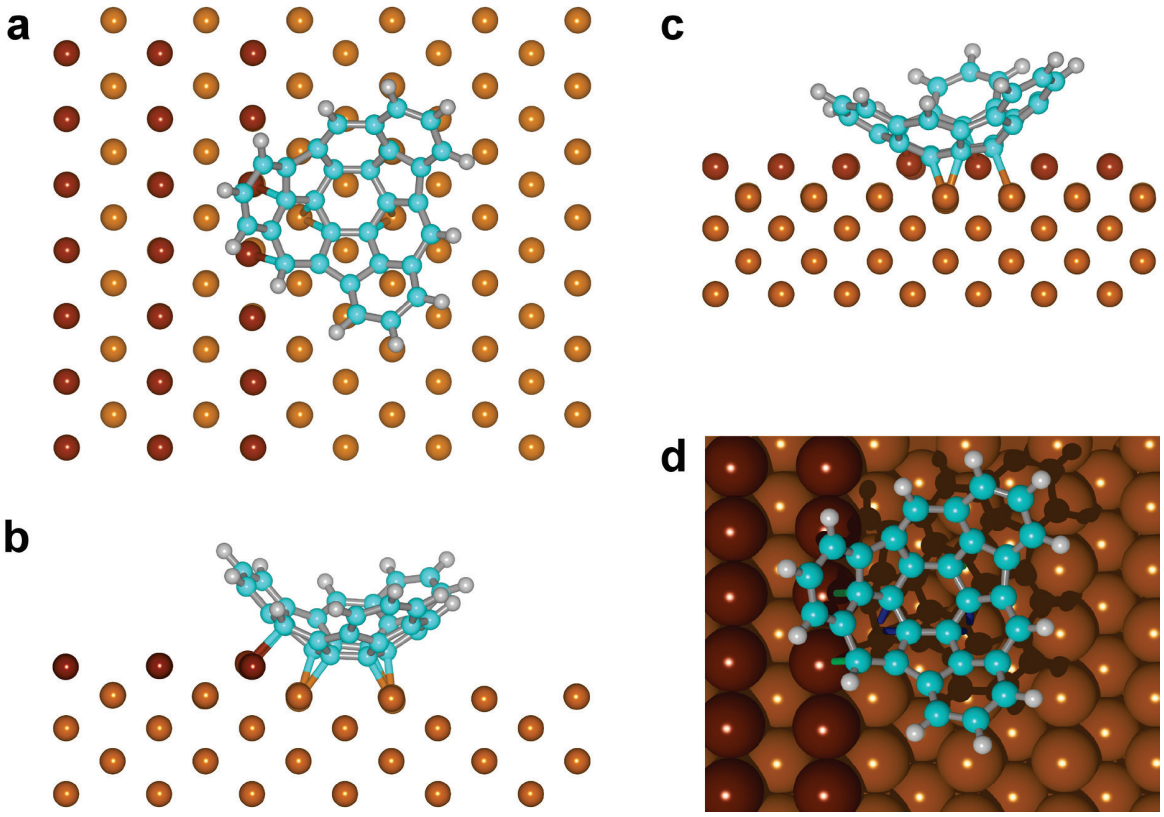

Supplementary Figure 8 | Optimized configuration of *M*-hemifullerene at the step edge along the $\langle\bar{1}10\rangle$ direction. The optimal configuration involves one η^1 – and two η^2 – coordinative bonds to the lower terrace and two η^1 – coordinative bonds to adjacent step edge atoms.

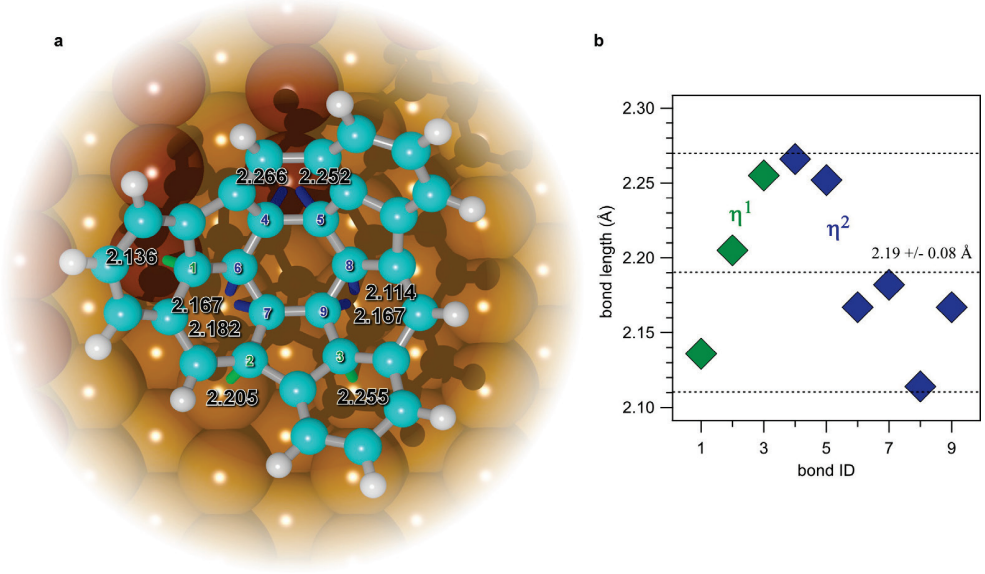

Supplementary Figure 9 | C-Cu bond length analysis for *M*-hemifullerene at the *R*-kink. (**a**) Perspective view (about 10° off a top view) showing all C-Cu bonds, highlighted in green (η^1 bonds) and blue (η^2 bonds). The bonds are labelled with a number on the corresponding C atom (bond ID). Bond

lengths as obtained from the DFT calculation are indicated. (**b**) Plot of the C-Cu bond lengths, with the average of 2.19 Å and the spread of ±0.08 Å indicated by dashed lines.

3) References

1. Fadley, C. S. *The Study of Surface Structures by Photoelectron Diffraction and Auger Electron Diffraction,* in *Synchrotron Radiation Research: Advances in Surface Science*, edited by R. Z. Bachrach (Plenum, New York, 1992), p. 421.
2. Fasel R. *et al.* Local structure of *c*(2×2)-Na on Al(001): Experimental evidence for the coexistence of intermixing and on-surface adsorption, *Phys. Rev. B* **50**, 14516-14524 (1994).
3. Fasel, R. *et al.* Orientation of Adsorbed C_{60} Molecules Determined via X-Ray Photoelectron Diffraction. *Phys. Rev. Lett.* **76**, 4733-4737 (1996).
4. Parschau, M. *et al.* Buckybowls on metal surfaces: Symmetry mismatch and enantiomorphism of corannulene on Cu(110). *Angew. Chem. Int. Ed.*, **46** 8258-8261 (2007).
5. Ivanic, J. & Ruedenberg, K. Rotation Matrices for Real Spherical Harmonics. Direct Determination by Recursion *J. Phys. Chem.* **100**, 6342-6347 (1996).
6. Wormington, M., Panaccione, C., Matney, K. M. & Bowen, D. K., Characterization of structures from X-ray scattering data using genetic algorithms. *Phil. Trans. R. Soc. Lond. A* **357**, 2827-2848 (1999).
7. http://www.igorexchange.com/project/gencurvefit.
8. IGOR Pro, WaveMetrics Inc., Lake Oswego, USA.